Experimental and Computational Study of CO2 Storage and Sequestration with Aqueous 2-Amino-2-hydroxymethyl-1,3-propanediol (TRIS) Solutions

ARTICLE *in* THE JOURNAL OF PHYSICAL CHEMISTRY A · NOVEMBER 2014

Impact Factor: 2.69 · DOI: 10.1021/jp5094959

3 AUTHORS:

Rama Oktavian
Brawijaya University
3 PUBLICATIONS **9** CITATIONS
SEE PROFILE

Mohamed Taha
University of Aveiro
50 PUBLICATIONS **324** CITATIONS
SEE PROFILE

Ming-Jer Lee
National Taiwan University of Science and Tec…
205 PUBLICATIONS **2,514** CITATIONS
SEE PROFILE

THE JOURNAL OF PHYSICAL CHEMISTRY A

Article

pubs.acs.org/JPCA

Experimental and Computational Study of CO_2 Storage and Sequestration with Aqueous 2-Amino-2-hydroxymethyl-1,3-propanediol (TRIS) Solutions

Rama Oktavian,[†] Mohamed Taha,*[,‡] and Ming-Jer Lee*[,†]

[†]Department of Chemical Engineering, National Taiwan University of Science & Technology, 43 Keelung Road, Section 4, Taipei 106-07, Taiwan

[‡]CICECO, Departamento de Química, Universidade de Aveiro, 3810-193 Aveiro, Portugal

ABSTRACT: Experimental solubility data of CO_2 in (5 and 10) mass% TRIS aqueous solutions were measured at (318.15 and 333.15) K and up to 10 MPa. The solubility data were well correlated with the modified Kent−Eisenberg model. The reaction mechanism, reaction energies, and equilibrium constants for the formation of bicarbonate and carbamate from CO_2, H_2O, and TRIS were studied using the quantum-chemical approach COSMO-RS (conductor-like screening model for real solvents) at the BP/TZVP level. The bicarbonate and carbamate formations were confirmed by using Fourier transform infrared (FTIR) spectroscopy. The results demonstrate that the formation of the bicarbonate anion is the main product formed by the direct reaction of CO_2 with water and TRIS, and reveal that the carbamate anion was formed by a proton transfer from TRIS−CO_2 zwitterion to TRIS. Density functional theory (DFT) calculations with transition-state optimization and intrinsic reaction coordinate (IRC) in water using IEF-PCM solvation model at the B3LYP/6-311++G(d,p) levels of theory were employed to support the reaction pathway for the bicarbonate and carbamate formations. The conversion of the absorption product to stable carbonate ($CaCO_3$) was also investigated experimentally by adding various Ca^{2+} sources, $CaCl_2{\cdot}2H_2O$ aqueous solution, and artificial seawater.

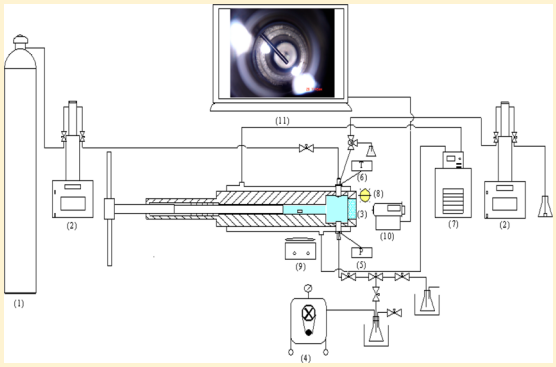

1. INTRODUCTION

Using fossil fuels as a primary energy source causes a significant increase in greenhouse gases, particularly CO_2 levels that lead to global warming effects.[1] The combustion of fossil fuels is known to contribute to 73% of CO_2 production.[2] Thus, finding a solution to minimize greenhouse gas emissions is a major research topic to address the global warming problem. According to the International Energy Agency's (IEA's) World Energy Outlook 2010 main scenario,[3] the projected growth in energy demand will translate into a 21% rise in energy-related CO_2 emissions between 2008 and 2035, mostly due to robust economic growth in developing countries. Therefore, the effort for mitigating global emission from CO_2 will be more challenging over the coming century.

Carbon capture and storage (CCS) represents one of the techniques proposed to reduce CO_2 levels. Currently, CO_2 capture technology is still facing some challenges regarding to the economic viability in the context of reducing greenhouse gas emission. Among CCS techniques, CO_2 aqueous absorption/stripping are the most common due to its low cost and simplicity.[4]

The most commonly used chemical solvents for CO_2 removal is amine-based solvents. The main advantage of these amine-based solvents is their fast reactivity due to the formation of stable carbamates, high CO_2 carrying capacity, low hydrocarbon solubility, and their relatively inexpensive price. However, they also have some drawbacks including that these solvents have high vapor pressure leading to emission during processing and their corrosive nature limits being used in dilute solution.[5] They also form degradation products due to the side reactions between some minor constituents of flue gas. Moreover, they have high reaction heat with CO_2 that leads to higher stripping energy consumption making it an expensive process.[6] Therefore, improvement of new absorbent for CO_2 removal process is very essential to address the issue.

Recently, there has been a great interest in using aqueous solutions, particularity of sterically hindered amines, for postcombustion CO_2 capture. Sterically hindered amines require less regeneration energy for CO_2 capture, in comparison with primary and secondary amines. It is attributed to the fast reaction rate of CO_2 with sterically hindered amines with CO_2 among the different classes of amines.[7] It also offers lower energy consumption in regeneration processing since sterically hindered amines form unstable carbamates and carbonate ions may be presented in the solution in greater amounts than carbamates ions.[8]

Received: September 19, 2014
Revised: November 10, 2014
Published: November 12, 2014

dx.doi.org/10.1021/jp5094959 | J. Phys. Chem. A 2014, 118, 11572−11582

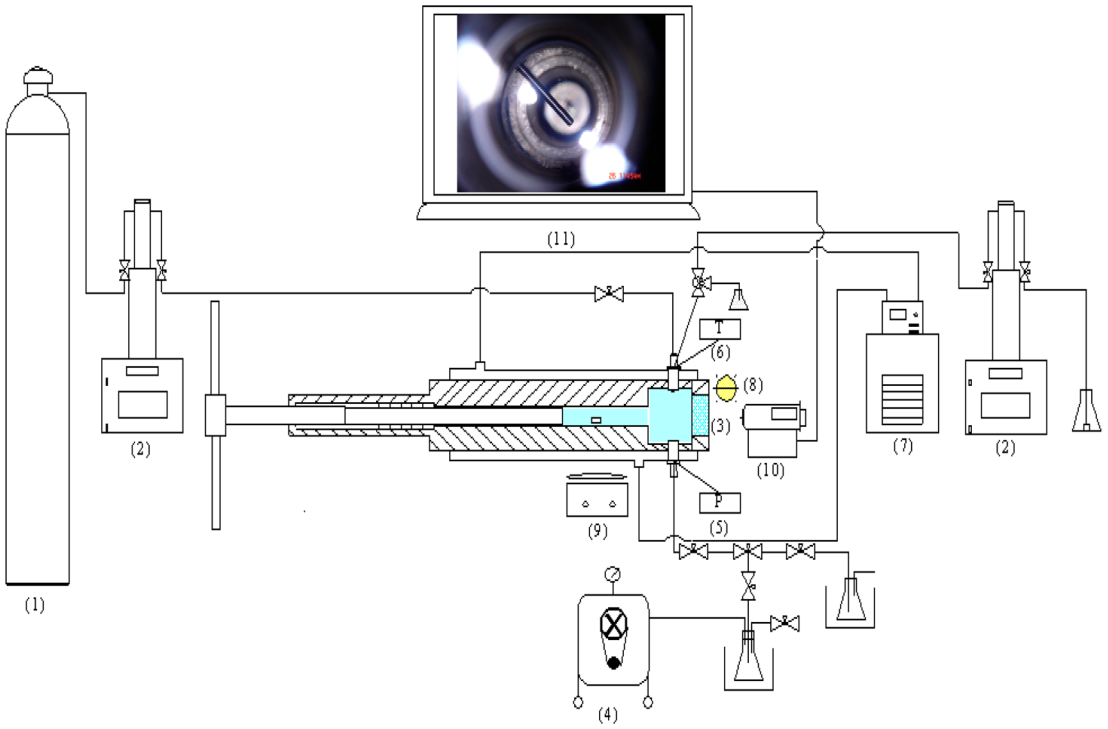

Figure 1. Schematic diagram of the Phase Equilibrium Analyzer (PEA) apparatus.

One of sterically hindered amines family that can be considered as a potential solvent for CO_2 absorption process is 2-amino-2-hydroxymethyl-1,3-propanediol, known as TRIS. TRIS consists of three hydroxyl groups and one amine group. Its application in CO_2 absorption process as a potential absorbent has been gaining interest in recent years. The solubility of CO_2 in (10 and 20) mass% of aqueous TRIS solutions was measured at (313.15, 323.15, and 333.15) K and partial pressures of CO_2 ranging from (1 to 2000) kPa, and the results showed that aqueous TRIS solution can be considered as potential CO_2 absorbent.[9] CO_2 solubility was also measured in 10 mass% of TRIS aqueous solution at 298.15 K and partial pressures of CO_2 ranging from (0.09 to 2427) kPa[10] and in solution with (0.0015, 0.005, 0.01, and 0.025) mass fraction with the addition of human carbonic anhydrase enzyme at 0.025 mass fraction at temperatures (283.15, 298.15, and 313.15) K for CO_2 partial pressures within (2 to 75) kPa. It was found that the addition of enzyme did not obviously affect the solubility of CO_2.[11] However, the phase equilibrium behavior of CO_2 in these aqueous solutions has not been fully investigated, and the solubility data are only available for limited range of experimental conditions. The CO_2 loading capacity of aqueous TRIS solutions was found to be higher than the industrially often used alkanolamine (monoethanolamine, MEA) especially at partial pressures higher than ~40 kPa.[10] While at lower partial pressures, the CO_2 loading capacity in the former solution is higher than the latter one.[10]

In the present study, we extended the experimental partial pressures of carbon dioxide up to about 11.76 MPa in (5 and 10) mass% of aqueous TRIS solutions at (318.15 and 333.15) K. The solubility data were correlated with the modified Kent–Eisenberg model.[11] COSMO-RS (Conductor-like Screening Model for Real Solvents)[12] and Fourier transform infrared (FTIR) analysis were conducted to explore the reaction mechanism underlying the CO_2 absorption products (bicarbonate and carbamate anions) in aqueous TRIS solutions. The reaction path of the bicarbonate and carbamate formations were further examined in more detail using DFT calculations with a polarizable continuum model (IEF-PCM) solvation model at the B3LYP/6-311++G(d,p) level of theory.

Following CO_2 capture by chemical absorption, it is then needed to be stored. Nowadays, geological storage of CO_2 has been gaining increasing attention and interest as a part of comprehensive CCS technology widely known as the sequestration process. There are a lot of possible approaches for the sequestration process of CO_2 being investigated by researchers worldwide.[13] The most common method used is chemical fixation of CO_2-forming carbonate minerals, which is considered as a permanent method of disposing CO_2 and also environmental friendly.[14] In this study we investigated the feasibility of the CO_2 sequestration process for absorbed solutions by using three different mineral precipitants.

2. EXPERIMENTAL SECTION

2.1. Materials. TRIS (CAS: 77-86-1), $CaCl_2 \cdot 2H_2O$ (CAS: 10035-04-8) and sea salt used in this study were purchased from Sigma-Aldrich with the purity of >99 mass%. Carbon dioxide (purity of 99.5 mass%) was supplied by Liu-Hsiang Co. (Taiwan). The deionized water was prepared by using a NANO pure-Ultra pure water system with resistivity of 18.3 MΩ cm, and deuterium oxide (D_2O, mass fraction purity = 0.998 atom D) was purchased from Acros Organics.

2.2. Solubility Measurements. The solubility data of CO_2 in TRIS aqueous solution at elevated pressures was measured by using a Phase Equilibrium Analyzer (PEA) based on a synthetic method that does not require the composition analysis described previously.[15] The schematic diagram of this apparatus is shown in Figure 1. This apparatus consists of a high-pressure generator (Model 62-6-10, High Pressure Equipment Co., USA) equipped with a sapphire window

dx.doi.org/10.1021/jp5094959 | J. Phys. Chem. A 2014, 118, 11572–11582

(Part No. 742.0106, Bridgman closure, SITEC, Switzerland), a rupture disk, and a circulation jacket. The internal volume of the cell can be adjusted manually from 35 cm^3 to 60 cm^3 with a piston screw pump, and the cell is operable up to 50 MPa and 473.15 K. The cell's temperature was controlled by circulated thermostatic water and was measured using an inserted thermocouple (TM-917 model), whose reading was calibrated previously to within an uncertainty of 0.1 K. A pressure transducer (PDCR 407-01, Druck, UK) with a digital display (DPI 280, Druck, UK) measured the cell's pressure to within an uncertainty of 0.04%.

The empty cell was purged several times with carbon dioxide to remove entrapped air. After evacuating the cell, two precision syringe pumps (model 260D, Isco Inc., USA) were used to charge carbon dioxide and TRIS solutions, respectively. The loaded mixture in the cell was compressed to the desired pressure by displacing the movable piston fitted within the cell. A magnetic stir bar was placed inside the cell to promote the mixing of the mixture. The weight of each loaded material was calculated from the known charged volume (accurate to ±0.01 cm^3) and its density at loaded pressure and temperature. While the densities of carbon dioxide were taken from the NIST Chemistry WebBook, those of the aqueous TRIS solutions were determined experimentally using a high-pressure densitometer (DMA 512P, Anton Paar, Austria) with an oscillation period indicator (DMA 48, Anton Paar, Austria) to an uncertainty of 0.0001 g cm^{-3}. The uncertainty of the composition of the prepared mixtures was estimated to be 0.003 in mole fraction. The phase behavior of the loaded mixture in the cell was observed with the aid of a digital camera (Model: DSC-F88/S, Sony, Japan), LED-white light, and a television (model SE2231R, BenQ, Taiwan). The loaded sample was compressed to form a single phase at a fixed temperature, and the mixture was maintained homogeneously for at least 20 min. The pressure was then slowly decreased until the second phase appeared by manually manipulating the position of piston screw pump. The uncertainty of the observed phase transition pressures was estimated to be 0.02 MPa. In case a small bubble appeared in the cell, a bubble point was obtained.

2.3. FTIR Measurements. The FTIR spectra were measured by a Bio-Rad Digilab FTS-3500 spectrometer at a spectral resolution of 4 cm^{-1} and 200 scans. The solutions were prepared by dissolving TRIS (10 mass%) in H_2O or D_2O. The solutions were saturated with CO_2 by bubbling from a cylinder at atmospheric pressure and pH is lowered (from 10.5 to 8.0). The pH was measured using A HTC-210U pH meter calibrated with pH 4.0 and 7.0 standard buffer solutions. The concentration of the bicarbonate anion in 1.0 M TRIS/D_2O produced by CO_2 bubbling was measured by FTIR measurements. For this propose, a calibration curve was made by dissolving several concentrations of $KHCO_3$ in D_2O. The bicarbonate concentration was obtained from the calibration curve, where the peak area of the C═O stretching band (1624 cm^{-1}) of the $KHCO_3$ was plotted as a function of $KHCO_3$ in the molarity unit. The samples were injected into an IR cell with two ZnSe windows (32 mm-diameter, Sigma-Aldrich) and an EZ-copper spacer (0.015 mm thick). The IR cell was maintained at 298.15 K. A background spectrum of the solvent was acquired at the beginning of the experiment. The IR spectra were collected and analyzed by the spectroscopic software Varian 4.10.

2.4. Computational Details. COSMO-RS is a powerful predictive thermodynamic model for fluid equilibria based on the results obtained from quantum chemical calculation of individual species combined with a statistical thermodynamics approach.[12] The use of the COSMO-RS model in predicting the properties of a wide variety of systems including CO_2-solvents has been demonstrated in several publications. The molecular geometries of all the species were optimized with the TURBOMOLE (ver. 6.1) program,[16] using the triple-ζ valence potential (TZVP) basis set[17] with the resolution of identity (RI) approximation[18] and the Becke and Perdew ($b-p$) functional[19] at the density functional theory (DFT) level. All of the compounds were optimized in gas phase and using the continuum solvation COSMO model to compute the necessary energy and COSMO files, respectively. These files were then used as inputs to COSMOtherm software (version C30_1401) for predicting thermodynamic properties.[12,20]

The pK_a values of TRIS and H_2CO_3 in water are predicted from the linear free energy relationship (LFER),[21] as implemented in the COSMOtherm program,

$$pK_a^i = c_0 + c_1(\Delta G^i_{neutral} - \Delta G^i_{ion}) \quad (1)$$

where $\Delta G^i_{neutral}$ and ΔG^i_{ion} are the Gibbs free energies of the neutral and the ionic compounds at infinite dilution in the solvent, respectively. In the case of H_2CO_3, the first pK_{a1} was calculated from the free energy difference of $G(H_2CO_3)-G(HCO_3^-)$, while the second pK_{a2} was computed from the free energy difference of $G(HCO_3^-) - G(CO_3^{2-})$. The LFER parameters c_0 and c_1 for water were read from the COSMOtherm parameter file.

The Gibbs free energies (ΔG_r), enthalpies (ΔH_r), and equilibrium constants (K_r) of the chemical reactions of CO_2 with TRIS in water at infinite dilution were calculated using the advanced feature of the latest released COSMOtherm, the parametrization BP_TZVP_ C30_1401, which was parametrized by considering the thermodynamic parameters (ΔG_r, ΔH_r, and K_r) of reaction. The ΔG_r of reaction is defined as the difference in the total Gibbs energies between the product compounds and the reactants, and the values for Gibbs energies of the reaction compounds are calculated from the DFT gas phase energies modified by the free energy of solvation (ΔG_{solv}) using COSMOtherm. The reaction equilibrium constant was calculated by

$$K_r = \exp(-\Delta G_r/RT) \quad (2)$$

where R is the gas constant. In a similar way, ΔH_r is the difference of the enthalpies of the product compounds and the reactants.

The reactants and products, as well as the transition state optimizations of the bicarbonate and carbamate formations in water, using the IEF-PCM solvation model, were analyzed at the DFT/B3LYP/6-311++G(d,p) level. The optimized geometries of the transition states were followed by IRC calculations. The Gaussian09 package[22] was used for the DFT calculations. The activation energies were calculated by the difference of the total energies between the transition state (E_{TS}) and reactants (E_R) for the forward reaction, and between the E_{TS} and products (E_P) for the inverse reaction, respectively. Vibration frequency computations were conducted to verify that the obtained geometries were minima or transition structures.

2.5. CO_2 Sequestration Process. The CO_2 sequestration process in this work was studied by precipitating a CO_2–

TRIS−water mixture into $CaCO_3$ solid using mineral precipitants. In this study, three different precipitants were used, including 2.5 M $CaCl_2$ aqueous solution, $CaCl_2{\cdot}2H_2O$ + TRIS aqueous solution, and artificial seawater (ASW). ASW was prepared by dissolving 3.8 g of Sigma artificial-seawater salts in 100 cm^3 of double distilled water. The CO_2−TRIS−water saturation mixture, 15 cm^3, collected from the PEA was introduced into a tightly closed, jacketed equilibrium cell. The temperature of the mixture in the cell was maintained at 308.15 and 328.15 K using thermostatic water circulated through the jacket. The mixture was stirred for approximately 8 h (until the pH of solution remained constant). After reaching equilibrium, 5 cm^3 of two precipitants and 10 cm^3 of ASW were added to the solution by titration method, and the mixture was left to precipitate for 15 min to make sure that all carbonate ions formed carbonate precipitate. The solution was then filtered with filter crush following the precipitation process. During the filtration process, the crush was washed several times with water and acetone to remove all impurities. The filter crush was then kept and dried in an oven for approximately 12 h to vaporize all water and impurities. The mass of $CaCO_3$ dried precipitate was determined using an analytical balance.

3. RESULTS AND DISCUSSION

3.1. Solubility Data and Correlation. The experimental solubility data of CO_2 in (5 and 10) mass% TRIS solution are presented in Tables 1, respectively, expressed as the mole fraction of CO_2 in the mixture. In addition, the solubility data expressed as a P−x diagram and the influence of temperature are also illustrated in Figure 2 at temperatures of 318.15 and 333.15 K for CO_2 in 5 and 10 mass% TRIS, respectively. The solubility of CO_2 in TRIS aqueous solutions decreases with increasing temperature. At a given CO_2 mole fraction, the equilibrium pressure increases with increasing of temperature. Also, at constant temperature and pressure, the solubility of CO_2 in TRIS aqueous solutions increases with increasing TRIS concentration of the solutions.

Table 1. Solubility Data of CO_2 in 5 and 10 mass% TRIS Aqueous Solutions at Temperatures of 318.15 and 333.15 K

	P (MPa)	
CO_2 in mole fraction	318.15 K	333.15 K
5 mass% TRIS		
0.0206	3.93	5.19
0.0238	5.05	6.57
0.0270	6.38	8.52
0.0303	7.69	9.52
0.0329	9.78	11.76
10 mass% TRIS		
0.0194	2.31	3.15
0.0239	3.78	5.04
0.0269	5.11	6.75
0.0298	6.62	8.57
0.0329	8.53	10.75

In this study, the modified Kent−Eisenberg model[11] was applied to correlate experimental solubility data since it is simple but applicable to correlating the solubility data for CO_2−alkanolamine aqueous systems.[7,11] This model was developed based on chemical theory, in which the system was assumed to be physically ideal (i.e., the activity coefficient and the fugacity coefficient of each species are unity) and the nonideality of system was lumped in the equilibrium constants of the chemical reactions taking place in the absorption of CO_2 by aqueous alkanolamine solutions. The model was further modified by expressing the equilibrium constants as a function of temperature, CO_2 loading, and the concentration of alkanolamine solutions.

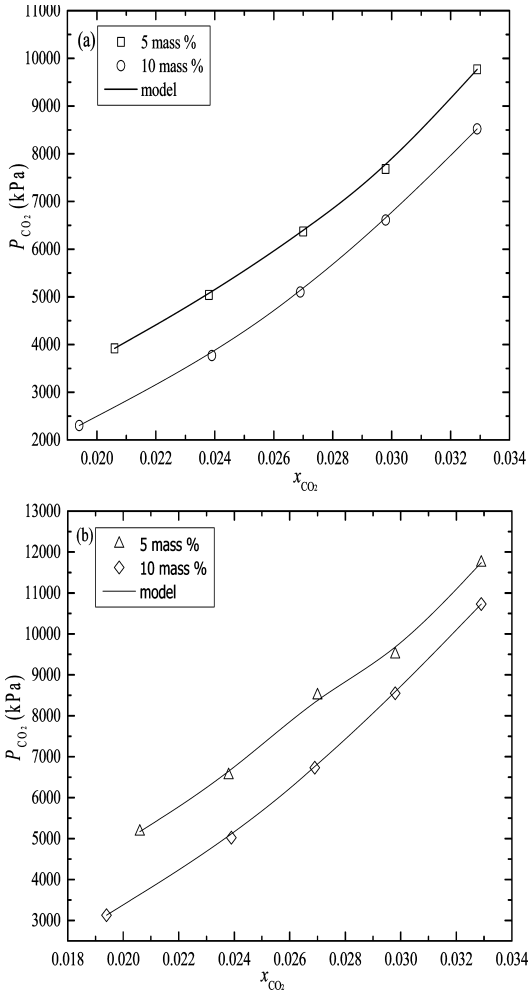

Figure 2. Solubilities of CO_2 in 5 and 10 mass% TRIS aqueous solutions at (a) 318.15 K and (b) 333.15 K.

In the CO_2−TRIS aqueous solution system, five chemical reactions may be involved, which are given as below.[11]

(1) The formation of carbamate ions:

$$RNH_2 + HCO_3^- \overset{K_1}{\leftrightarrow} RNHCOO^- + H_2O, \quad K_1 = \frac{[RNHCOO^-]}{[RNH_2][HCO_3^-]} \tag{3}$$

(2) The deprotonation of the amine group:

$$RNH_3^+ \overset{K_2}{\leftrightarrow} RNH_2 + H^+, \quad K_2 = \frac{[RNH_2][H^+]}{[RNH_3^+]} \tag{4}$$

(3) The formation of bicarbonate:

$$CO_2 + H_2O \overset{K_3}{\leftrightarrow} HCO_3^- + H^+, \quad K_3 = \frac{[HCO_3^-][H^+]}{[CO_2]} \tag{5}$$

(4) The dissociation of bicarbonate:

dx.doi.org/10.1021/jp5094959 | J. Phys. Chem. A 2014, 118, 11572−11582

Table 2. Values of the Parameters for Calculating the Equilibrium Constants[a]

i	equilibrium constant for reaction i	a_{i1}	$10^{-3}\ a_{i2}$	$10^{-8}\ a_{i3}$	a_{i4}	a_{i5}	a_{i6}	a_{i7}
1	K_1 (mol/L)$^{-1}$	6.51	7.58	3.78	−0.60	3.88	−0.986	0.986
2	K_2 (mol/L)	13.5	adjust.	adjust.	adjust.	−3.60	−2.250	0.033
i	equilibrium constant for reaction i	b_{i1}	$10^{-4}\ b_{i2}$	$10^{-8}\ b_{i3}$	$10^{-11}\ b_{i4}$		$10^{-13}\ b_{i5}$	
3	K_3 (mol/L)	−241.818	29.8253	−1.48528	0.332648		−0.282393	
4	K_4 (mol/L)	−294.74	36.4385	−1.84158	0.415793		−0.354291	
5	K_5 [(mol/L)^2]	39.5554	−9.879	0.568827	−0.146451		0.136146	

[a]The values of the parameters a_{il} were taken from Le Tourneux et al.[11] and b_{il} from Kent and Eisenberg.[23]

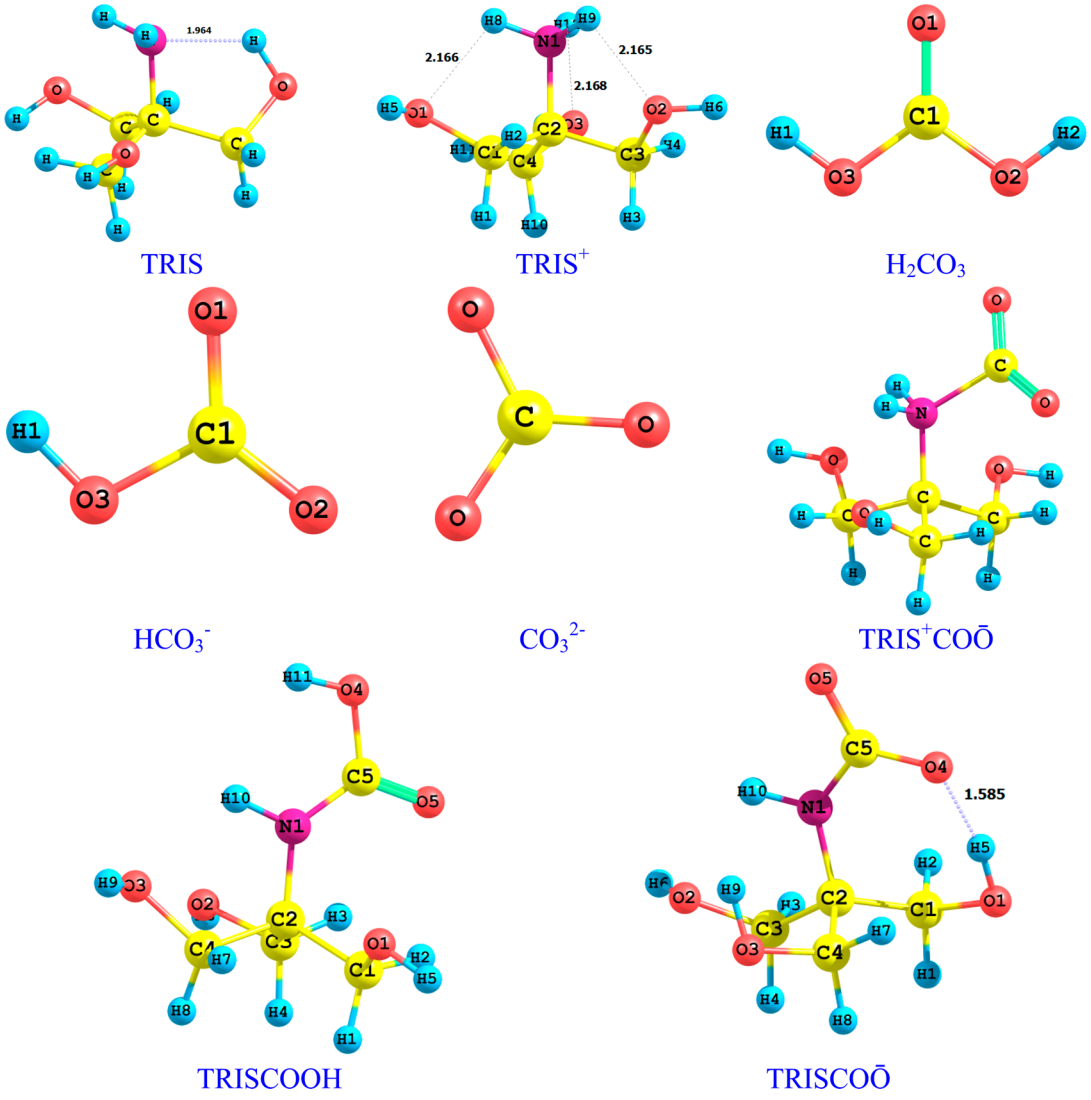

Figure 3. Optimized geometries of TRIS and H_2CO_3 equilibrium species with the lowest energy found at The DFT/TZVP levels. The atom distances are in angstroms.

$$HCO_3^- \overset{K_4}{\leftrightarrow} CO_3^{2-} + H^+, \quad K_4 = \frac{[CO_3^{2-}][H^+]}{[HCO_3^-]} \tag{6}$$

(5) The autoprotolysis of water:

$$H_2O \overset{K_5}{\leftrightarrow} H^+ + OH^-, \quad K_5 = [H^+][OH^-] \tag{7}$$

The concentrations of the eight species, $[RNHCOO^-]$, $[RNH_2]$, $[HCO_3^-]$, $[RNH_3^+]$, $[H^+]$, $[CO_2]$, $[CO_3^{2-}]$, and $[OH^-]$, involved in the above chemical reactions can be solved from the chemical equilibrium constants (K_1 to K_5) together with mass and charge balance equations:

$$m = [RNH_2] + [RNHCOO^-] + [RNH_3^+] \tag{8}$$

$$m\alpha = [RNHCOO^-] + [HCO_3^-] + [CO_3^{2-}] + [CO_2] \tag{9}$$

$$[H^+] + [RNH_3^+] = [RNHCOO^-] + [HCO_3^-] + 2[CO_3^{2-}] + [OH^-] \tag{10}$$

where m is the TRIS aqueous solution molarity expressed in mol L^{-1} and α is carbon dioxide loading, which is defined as the

dx.doi.org/10.1021/jp5094959 | J. Phys. Chem. A 2014, 118, 11572−11582

number of moles CO_2 absorbed per mol of TRIS. The relationship between α and m is given by eq 9. The partial pressure of carbon dioxide is then obtained by means of Henry's law:

$$p_{CO2} = H_{CO2}[CO_2] \tag{11}$$

where H_{CO2} is the Henry's constant of carbon dioxide in the aqueous solution, which was estimated from the following equation:[11]

$$H_{CO2}(\text{kPa·m}^3\text{·kmol}^{-1}) = 2.8249 \times 10^6 \exp[-2044/T(\text{K})] \tag{12}$$

The chemical equilibrium constants K_1 and K_2 are assumed as a function of temperature, CO_2 loading, and TRIS molarity:

$$\ln K_i = a_{1i} + a_{2i}/T + a_{3i}/T^2 + a_{4i}\alpha + a_{5i}/\alpha + a_{6i}/\alpha^2 + a_{7i}\ln(m) \tag{13}$$

while the equilibrium constants K_3, K_4, and K_5 are represented as a function of temperature only:

$$\ln K_i = b_{1i} + b_{2i}/T + b_{3i}/T^2 + b_{4i}/T^3 + b_{5i}/T^4 \tag{14}$$

The values of the parameters a_{j1} (j from 1 to 7), a_{j2} (j = 1, 5 to 7) and b_{k3}, b_{k4}, b_{k5} (k from 1 to 5) were taken from literatures and summarized in Table 2. The variables a_{j2} (j from 2 to 4) are adjustable parameters, which were determined by minimization of the following objective function (π):

$$\pi = \frac{1}{n}\sum_{i=1}^{n} |(p_{CO2})_i^{calc} - (p_{CO2})_i^{expt}|/(p_{CO2})_i^{expt} \tag{15}$$

where n is the number of data points, and the superscripts "calc" and "expt" denote the calculated and experimental values, respectively. With the aid of Matlab software, the optimized values of a_{22}, a_{32}, and a_{42} are found by using Nelder–Mead simplex method. Equation 16 presents the best-fit result for K_2:

$$\ln K_2 = 13.5 + 1.00 \times 10^3/T + 1.0105 \times 10^8/T^2 + 0.9499\alpha - 0.360/\alpha - 2.250/\alpha^2 + 0.033\ln(m) \tag{16}$$

The calculated results are compared with the experimental values in Figure 2, indicating that the agreement is satisfactory and the modified Kent–Eisenberg model is applicable to the CO_2-TRIS aqueous solution system for this study.

3.2. Ab Initio Calculations. The first phase in our theoretical calculation of understanding the CO_2-absorption using aqueous solution of TRIS was the determination of the pK_a^{COSMO} values of TRIS and H_2CO_3 from the LFER method using COSMOtherm. The DFT/TZVP optimized geometries of the neutral and protonated forms of TRIS and H_2CO_3 equilibrium species are shown in Figure 3. TRIS molecule contains an amine and three hydroxyl functional groups that are capable of forming hydrogen bonds. It was found that the N···H–O intramolecular H-bonding energy of the neutral alkanolamine is lower than that of O···H–N hydrogen bonding.[24] The neutral conformer of TRIS formed N···H–O intramolecular H-bonding, and thus it dominates the equilibrium population (Figure 3). On the other side, the protonated alkanolamine with an O···H–N intramolecular H-bonding has the lowest energy.[24] The O···H–N intramolecular H-bond lengths of the protonated TRIS are also shown in Figure 3. The computed pK_a^{COSMO} value of TRIS is 8.52, which agrees well with the experimental value, pK_a^{expt} = 7.81.[25] The pK_{a1}^{COSMO} and pK_{a2}^{COSMO} values are 3.02 and 9.67, whereas the corresponding pK_{a1}^{expt} and pK_{a2}^{expt} values are 3.72 and 10.35,[26] respectively, all in agreement with the experimental values. These two sets of predictions display the reliability of the theoretical method used.

Many theoretical studies have been conducted to understand the amine-CO_2–H_2O chemistry.[27] The chemical absorption of CO_2 using aqueous solution of alkanolamine occurs by the formation of carbamate and bicarbonate anions. The second phase in our calculation of the CO_2-capturing mechanism involved the determination of the Gibbs free energies (ΔG_r), enthalpy energies (ΔH_r), and equilibrium constants (K_r) for carbamate and biocarbonate formations.

The carbamate anion can be formed by two possible routes through a zwitterion carbamate as given below.[27g]

$$RNH_2 + CO_2 \leftrightarrow RNH_2^+COO^- \tag{17}$$

In the first route, the carbamate formation occurs by transferring a proton from the zwitterion carbamate to a TRIS molecule,

$$RNH_2^+COO^- + RNH_2 \leftrightarrow RNHCOO^- + RNH_3^+ \tag{18}$$

In the second route, the zwitterion carbamate was catalyzed by a water molecule to form carbamic acid, which subsequently reacts with another amine molecule forming carbamate as shown below:

$$RNH_2^+COO^- + H_2O \leftrightarrow RNHCOOH + H_2O \tag{19}$$

$$RNHCOOH + RNH_2 \leftrightarrow RNHCOO^- + RNH_3^+ \tag{20}$$

The bicarbonate anion may be formed from the reaction between water and CO_2 molecules, where the amine molecule acts as a base, as shown in eq 21.

$$RNH_2 + CO_2 + H_2O \leftrightarrow HCO_3^- + RNH_3^+ \tag{21}$$

Moreover, the bicarbonate anion can be liberated by the hydrolysis of the carbamate anion because of the instability of the latter anion.

$$RNHCOO^- + H_2O \leftrightarrow HCO_3^- + RNH_2 \tag{22}$$

The optimized geometries of the zwitterion carbamate ($TRIS^+COO^-$), carbamic acid (TRISCOOH), and carbamate ($TRISCOO^-$) are shown in Figure 3. The TRIS carbamate anions showed an $NCOO^-$···H–O intramolecular H-bond. The computed reaction energies (ΔG_r and ΔH_r), as well as the equilibrium constants (log K_r) for the formation of bicarbonates and carbamates (eqs 17–22) at different temperatures (298.15, 318.15, and 333.15 K) are reported in Table 3. The tabulated values show that the effect of temperature on ΔG_r, ΔH_r, and log K_r are small. The ΔG_r values for all reactions are negative, indicating that the equilibria are shifted significantly toward the product side. The bicarbonate formation via the direct reaction of CO_2, H_2O, and TRIS (eq 21) shows the lowest free energy, and lower than the carbamate obtained from reaction between the zwitterion carbamate and TRIS, by 3.19 kcal·mol^{-1}. It is suggested that the bicarbonate formation is dominant over the carbamate formation, and this can be seen from their equilibrium constants, in which the log K_r of the latter (log K_r = 10.62) is lower than that of the former (log K_r = 12.96). Although the equilibrium constant of the carbamate formation (log K_r = 9.19) through the proton transfer from TRISCOOH to TRIS molecule is relatively high,

dx.doi.org/10.1021/jp5094959 | J. Phys. Chem. A 2014, 118, 11572–11582

Table 3. Calculated Free Energies (kcal·mol^{-1}), Enthalpies (kcal·mol^{-1}), and Equilibrium Constants of the Reactions (Eqs 17−22)

		298.15 K				318.15 K				333.15 K			
eq	reaction	ΔG_r	ΔH_r	K_r	log K_r	ΔG_r	ΔH_r	K_r	log K_r	ΔG_r	ΔH_r	K_r	log K_r
17	TRIS + CO_2 ↔ $TRIS^+COO^-$	−2.50	−1.69	68.14	1.83	−2.58	−1.36	59.34	1.77	−2.64	−1.04	54.33	1.74
18	$TRIS^+COO^-$ + TRIS ↔ $TRISCOO^-$ + $TRIS^+$	−14.49	−25.04	4.21×10^{10}	10.62	−13.55	−24.32	2.03×10^9	9.31	−12.89	−23.66	2.84×10^8	8.45
19	$TRIS^+COO^-$ + H_2O ↔ TRISCOOH + H_2O	−1.96	−3.81	27.44	1.44	−1.73	−3.57	15.36	1.19	−1.56	−3.37	10.51	1.02
20	TRISCOOH + TRIS ↔ $TRISCOO^-$ + $TRIS^+$	−12.53	−21.24	1.53×10^9	9.19	−11.82	−20.74	1.32×10^8	8.12	−11.33	−20.29	2.70×10^7	7.43
21	TRIS + CO_2 + H_2O ↔ HCO_3^- + $TRIS^+$	−17.68	−29.83	9.17×10^{12}	12.96	−16.65	−28.61	2.74×10^{11}	11.44	−15.93	−27.51	2.83×10^{10}	10.45
22	$TRISCOO^-$ + H_2O ↔ HCO_3^- + TRIS	−0.69	−3.10	3.20	0.51	−0.52	−2.94	2.27	0.36	−0.40	−2.81	1.84	0.26

the existence of the TRISCOOH is low as observed from its equilibrium constant (log K_r = 1.44). The log K_r of the carbamet hydrolysis, eq 22, is low, and therefore, it does not seem that the carbamate species undergo hydrolysis to produce bicarbonate species.

The solvation free energy of (ΔG_{solv}) of $TRIS^+COO^-$ and $TRISCOO^-$ are −10.53 and −66.45 kcal·mol^{-1}, respectively. The ΔG_{solv} of TRIS and $TRIS^+$ are −8.50 and −50.68 kcal·mol^{-1}, respectively. Thus, the dramatic change of the hydration of the carbamate anions and the protonated amine ($TRIS^+$) is the driving force of the carbamate and bicarbonate formations.

The CO_2 absorption pathway of carbamate formation through eq 18 and the direct bicarbonate formation (eq 21) were further investigated by the transition-state optimization and IRC calculation in water at the DFT/IEF-PCM/B3LYP/6-311G++(d,p) level. The stable conformations of the optimized transition states, reactants, and products, as well as the IRC calculations of both reactions are shown in Figures 4 and 5. The results reveal that intermolecular hydrogen bonds are favorable even in the solvent. In Figure 4, three intermolecular hydrogen bonds formed within the reactant ($TRIS^+COO^-$ + TRIS) or the product ($TRISCOO^-$ + $TRIS^+$) of the carbamate formation (eq 18), and the transition state (TS_{18}) was stabilized by an intermolecular hydrogen bond [(TRIS) CO−H···$^-$OCO-($TRISCOO^-$)]. The activation energy of the carbamate formation is quite low (∼2.3 kcal·mol^{-1}), suggesting that the carbamate zwitterion is easily deprotonated by TRIS to produce a carbamate anion.

In the geometry of the reactants of the direct bicarbonate formation (Figure 5), an intermolecular H-bond between the nitrogen atom of TRIS and hydrogen atom of water was observed. The transition state (TS_{21}) of this reaction shows an intermolecular hydrogen bond between a hydrogen of a hydroxyl group of TRIS with an oxygen atom of the bicarbonate anion [(TRIS) CO−H···$^-$OCOOH]. In the product, two intermolecular hydrogen bonds are found. The first one is formed between a hydrogen of the protonated amine group of TRIS and the oxygen atom of the hydroxyl group of bicarbonate anion [(TRIS)N···H−$OCOO^-$], and the second one is the [(TRIS) CO−H···$^-$OCOOH] type. The calculated activation energy for the direct bicarbonate formation, eq 21, is ∼11 kcal·mol^{-1}. The energy barrier for the inverse reaction of the carbamate formation is ∼5.5 kcal·mol^{-1}, which is lower than that of the direct bicarbonate formation (∼12.4 kcal·mol^{-1}). Therefore, these results indicate that the bicarbonate anion dominates in the TRIS−H_2O−CO_2 system.

3.3. FTIR Analysis. FTIR analysis was also made to investigate the bicarbonate and carbamate formations in TRIS + CO_2 + H_2O system, and the results are depicted in Figure 6. The FTIR spectra of 10 mass% TRIS aqueous solution show a characteristic vibration mode at 1643 cm^{-1} due to N−H bending. The C−O and C−N stretching modes appear at 1041 and 1080 cm^{-1}, respectively. The peak at 1465 cm^{-1} is due to $-CH_2$ bending. On the other hand, the FTIR spectra of 10 mass% TRIS aqueous solution + CO_2 reveal significant changes induced by CO_2 absorption. The peak of the dissolved CO_2 is observed at 2342 cm^{-1}, which is in excellent agreement with the literature values of 2342, 2343.5, and 2343 cm^{-1}.[28] The resulting spectra (Figure 6a) indicate that the bicarbonate species is dominant, and show peaks at 1361 cm^{-1} (−CO$\bar{O}$ stretching) and 1303 cm^{-1} (C−OH bending), which are similar to the values reported by other investigators.[26,29] The C═O

dx.doi.org/10.1021/jp5094959 | J. Phys. Chem. A 2014, 118, 11572−11582

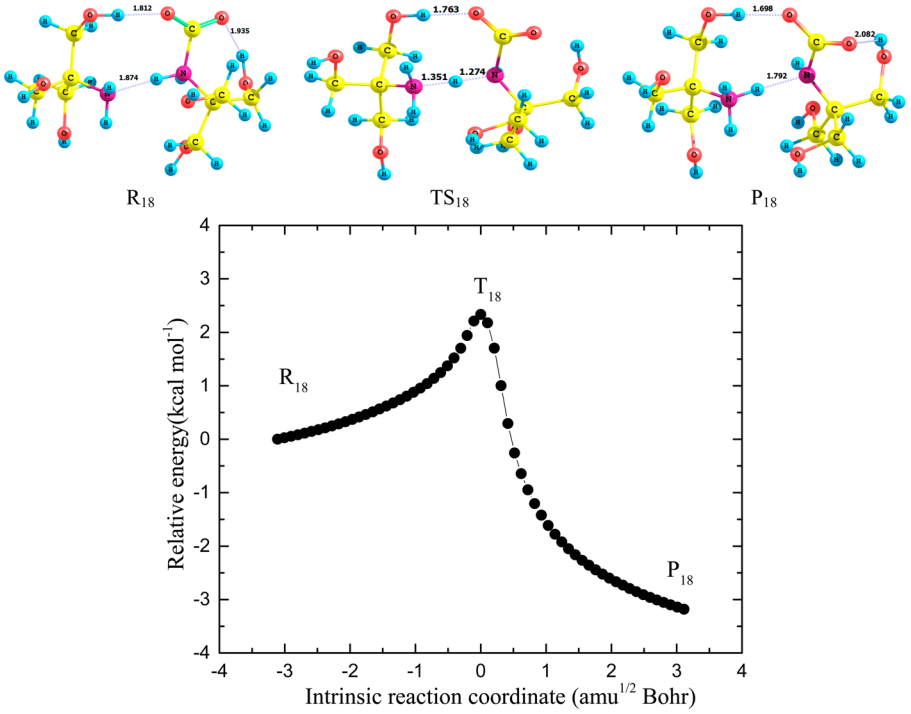

Figure 4. Stable conformations of the optimized transition states (TS_{18}), reactants (R_{18}: $TRIS^{+}CO\bar{O}$ + TRIS), and products (P_{18}: $TRISCO\bar{O}$ + $TRIS^{+}$), as well as the IRC calculation of the carbamate formation through eq 18, at the DFT/IEF-PCM/B3LYP/6-311G++(d,p) levels.

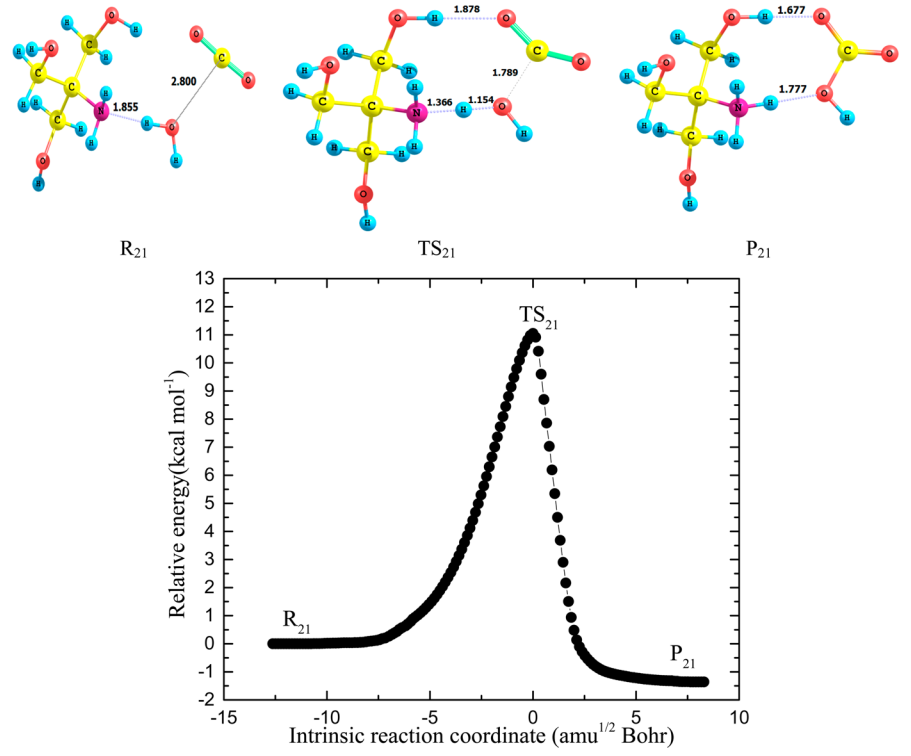

Figure 5. Stable conformations of the optimized transition states (TS_{21}), reactants (R_{21}: TRIS + H_2O + CO_2), and products (P_{21}: HCO_3^- + $TRIS^{+}$), as well as the IRC calculation of the bicarbonate formation through eq 21, at the DFT/IEF-PCM/B3LYP/6-311G++(d,p) levels.

stretching band of the bicarbonate at 1634 cm^{-1} [26,29] is strongly overlapped with TRIS N−H bending. In addition, the C−OH stretching peak at 1014 cm^{-1} [26,29] of the bicarbonate is also overlapped with both the C−O and the C−N stretching bands of TRIS. To confirm the existence of the C═O stretching band of the bicarbonate, we also performed all the FTIR measurements in D_2O solutions. The TRIS N−H bending band at 1643 cm^{-1} is shifted to about 1462 cm^{-1} in D_2O due to the deuteration (H/D exchange), as shown in Figure 6b. A broad peak in 1300 cm^{-1} region is due to a significant contribution of $-CH_2$ and C−C stretching of TRIS in D_2O, and the band at 1141 cm^{-1} arising from C−N stretching. The C═O stretching

dx.doi.org/10.1021/jp5094959 | J. Phys. Chem. A 2014, 118, 11572−11582

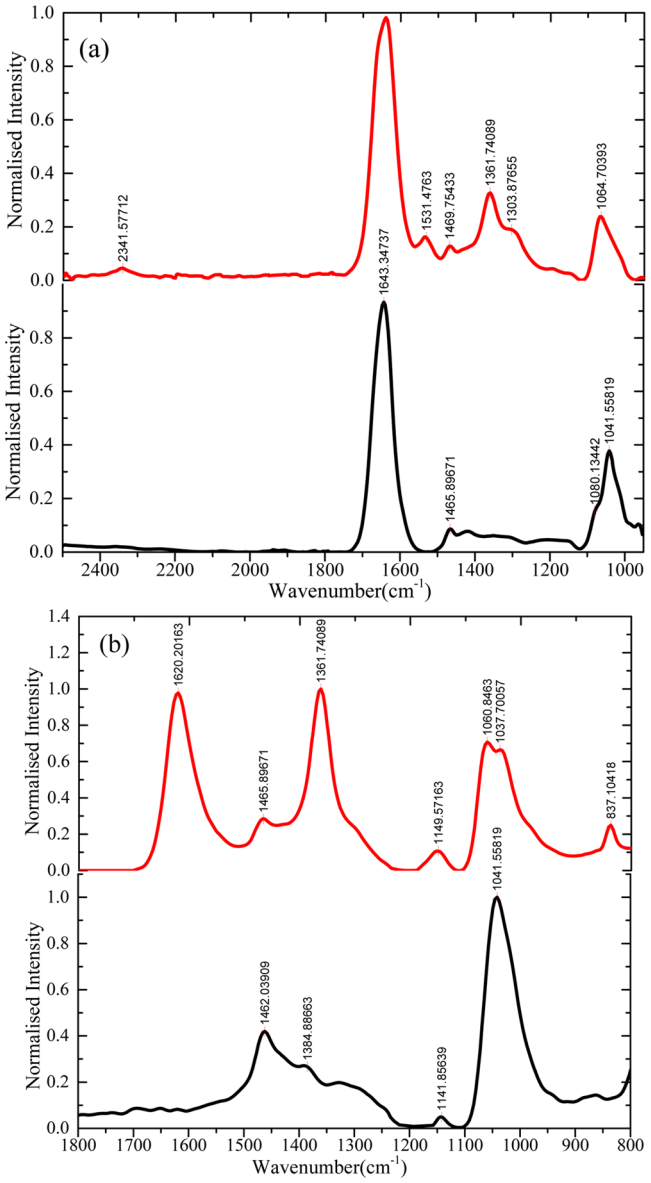

Figure 6. FTIR spectra of (a) 10 mass% TRIS + CO_2 + H_2O system and (b) 10 mass% TRIS + CO_2 + D_2O system. The black lines refer to CO_2-free solutions (10 mass% TRIS+ H_2O/D_2O), and red lines present TRIS + CO_2 + H_2O/D_2O mixtures.

band of the bicarbonate, formed in TRIS + D_2O solution, appears at 1624 cm^{-1}. This band and the other bands of the bicarbonate (1361, 1037 and 837 cm^{-1}) are in good agreement with previously reported values.[29] The small band at 1531 cm^{-1} is due to the carbamate (COO^-) asymmetric stretching, suggesting that the carbamate is formed in low concentration region.[30] The concentration of the formed bicarbonate in 1 M TRIS/D_2O was measured by FTIR analysis. The result shows that 0.60 mol of HCO_3^- was formed by CO_2 absorption in one mole TRIS/D_2O solution. It is important to notice that when bicarbonate formation is dominant, one mole of TRIS reacts with one mole of CO_2, while two moles of TRIS are needed to react with one mole of CO_2 for carbamate formation. Therefore, the FTIR measurements indicate that the bicarbonate anion is the main product in the CO_2−TRIS−water system.

3.4. CO_2 Sequestration Process. The effect of temperature on the formation of $CaCO_3$ was studied by setting the temperatures at 308.15 and 328.15 K, respectively. In this study, we also investigated the effect of the precipitants addition in the solution pH related to carbonate formation. The results of the precipitation experiments are summarized in Table 4 along with the pH measurement of solution after precipitation process. The amount of $CaCO_3$ formation decreases as temperature increases in both TRIS solutions because the solubility of carbon dioxide in the aqueous solutions decreases with increasing temperature.[14] The mixture of $CaCl_2.2H_2O$ + TRIS aqueous solution precipitant gives the highest amount of solid carbonate formation, with weight of 0.26 and 0.65 g at 308.15 K from the 15 cm^3 of 5 mass% and 10 mass% of TRIS solutions with saturated CO_2, respectively, and produces 0.16 and 0.36 g carbonates at 328.15 K, respectively. A minor amount of solid carbonate (only 0.0008 g) was obtained when artificial seawater was used due to the low amount of calcium ions contained in the seawater. The amount of carbonate formed after precipitation is presented in Figure 7 for CO_2 in 5 mass% TRIS solution and CO_2 in 10 mass% TRIS solution.

4. CONCLUSION

This study successfully measured the solubility of CO_2 in 5 and 10 mass% TRIS aqueous solution using the Phase Equilibrium Analyzer (PEA) apparatus at 318.15 and 333.15 K and at pressures up to 10 MPa. The solubility of CO_2 in TRIS aqueous solution decreases with increasing temperature and increases with increasing TRIS concentration. The modified Kent−Eisenberg model correlated satisfactorily the solubility data of CO_2 in TRIS aqueous solutions over the entire experimental conditions. The COSMO-RS at the BP/TZVP level was used to calculate the Gibbs free energies (ΔG_r), enthalpy energies (ΔH_r), and equilibrium constants (K_r) for carbamate and biocarbonate formations, as well as the protonation constants of TRIS and carbonic acid. FTIR analysis was also conducted to investigate the bicarbonate

Table 4. Results of Precipitation Experiments

		2.5 M $CaCl_2{\cdot}2H_2O$ + w % (w/w) TRIS[a]		2.5 M $CaCl_2{\cdot}2H_2O$		artificial seawater (ASW) (10 cm^3)	
CO_2[sat] solution of w % (w/w) TRIS[a]	T/K	$pH_{filtrate}$	$CaCO_3$/g	$pH_{filtrate}$	$CaCO_3$/g	$pH_{filtrate}$	$CaCO_3$/g
w = 5							
	308.15	7.20 ± 0.08	0.26 ± 0.02	5.75 ± 0.04	0.24 ± 0.02	7.90 ± 0.02	0.008 ± 0.001
	328.15	7.50 ± 0.05	0.16 ± 0.02	7.30 ± 0.05	0.15 ± 0.04	8.00 ± 0.07	0.009 ± 0.001
w = 10							
	308.15	6.50 ± 0.05	0.65 ± 0.02	5.60 ± 0.05	0.44 ± 0.02	7.90 ± 0.05	0.008 ± 0.001
	328.15	7.40 ± 0.05	0.36 ± 0.02	7.85 ± 0.05	0.21 ± 0.02	7.90 ± 0.05	0.009 ± 0.001

[a] w = mass percentage.

dx.doi.org/10.1021/jp5094959 | J. Phys. Chem. A 2014, 118, 11572−11582

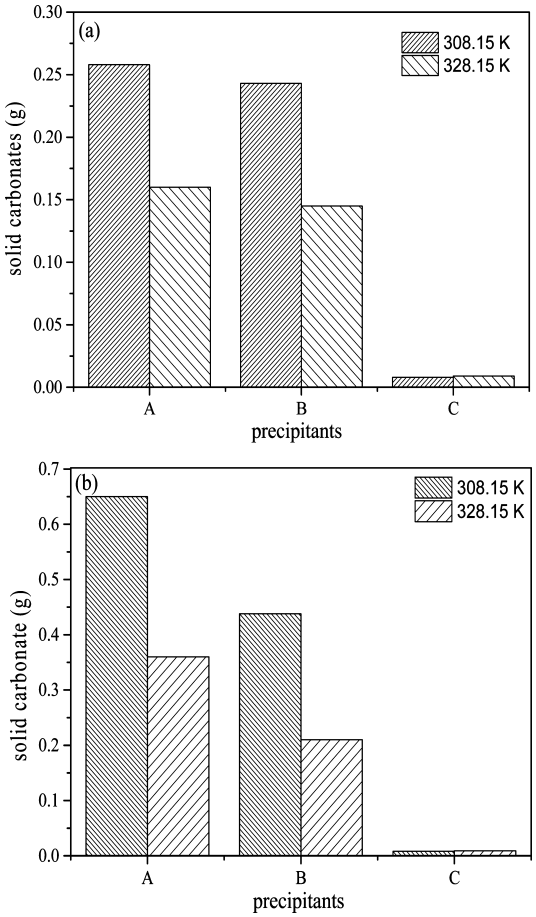

Figure 7. (a) Precipitation of CO_2 mixture with (a) 5 mass% TRIS and (b) 10 mass% TRIS: (A) $CaCl_2{\cdot}2H_2O$ + 5 mass% TRIS; (B) $CaCl_2{\cdot}2H_2O$; (C) artificial seawater.

and carbamate formations. As evidence from the results of calculated reaction energies and FTIR analysis, it is favorable to the bicarbonate formation through a single-step reaction. The carbamate formation is likely to proceed by transferring a proton from the TRIS-CO_2 zwitterion to a TRIS molecule, and hardly undergoes hydrolysis to form the bicarbonate. TRIS is more likely to act as a good proton acceptor in both carbonate and carbamate formations. We further implemented intrinsic reaction coordinate (IRC) calculations in the aqueous phase using (IEF-PCM) solvation model at DFT−B3LYP/6-311++G(d,p) levels of theory for the carbamate and bicarbonate formations. The CO_2 sequestration process was successfully conducted using three different precipitants ($CaCl_2{\cdot}2H_2O$ + TRIS aqueous solution mixture, $CaCl_2{\cdot}2H_2O$ aqueous solution, and artificial seawater) at 308.15 and 328.15 K. Those three precipitants demonstrated a feasible use as precipitant by producing solid carbonate. The amount of solid carbonate formation from both two CO_2-TRIS aqueous solutions decreases as temperature increases.

AUTHOR INFORMATION

Corresponding Authors

*E-mail: mtaha978@yahoo.com (M.T.).

*Tel.:+886 2 2737 6626; fax:+886 2 2737 6644. E-mail: mjlee@mail.ntust.edu.tw (M.-J.L.).

Notes

The authors declare no competing financial interest.

ACKNOWLEDGMENTS

The authors gratefully acknowledge the financial support from the Ministry of Science and Technology, Taiwan, through Grant No. NSC99-2214-E-011-079-MY3 and the international student scholarship provided by National Taiwan University of Science & Technology. M.T. acknowledges Fundação para a Ciência e Tecnologia for the postdoctoral grants SFRH/BPD/76850/2011 and SFRH/BPD/78441/2011, respectively. The authors also thank Dr. Ho-mu Lin for valuable discussions.

REFERENCES

(1) Yu, J.; Corripio, A. B.; Harrison, D. P.; Copeland, R. J. Analysis of the sorbent energy transfer system (SETS) for power generation and CO_2 capture. *Adv. Env. Res.* **2003**, *7* (2), 335−345.

(2) Wildenborg, T.; Lokhorst, A. Introduction on CO_2 geological storage-classification of storage options. *Oil. Gas Sci. Technol.* **2005**, *44*, 93−108.

(3) EIA, *International Energy Outlook*, 2010.

(4) (a) Hook, R. J. An investigation of some sterically hindered amines as potential carbon dioxide scrubbing compounds. *Ind. Eng. Chem. Res.* **1997**, *36* (5), 1779−1790. (b) Ma'mun, S.; Dindore, V. Y.; Svendsen, H. F. Kinetics of the reaction of carbon dioxide with aqueous solutions of 2-((2-aminoethyl)amino)ethanol. *Ind. Eng. Chem. Res.* **2007**, *46* (2), 385−394.

(5) Dash, S. K.; Samanta, A. N.; Bandyopadhyay, S. S. (Vapour liquid) equilibria (VLE) of CO_2 in aqueous solutions of 2-amino-2-methyl-1-propanol: New data and modelling using eNRTL-equation. *J. Chem. Thermodyn.* **2011**, *43* (8), 1278−1285.

(6) Liu, Y.; Zhang, L.; Watanasiri, S. Representing vapor−liquid equilibrium for an aqueous MEA−CO_2 system using the electrolyte nonrandom-two-liquid model. *Ind. Eng. Chem. Res.* **1999**, *38* (5), 2080−2090.

(7) Wang, C. W.; Soriano, A. N.; Yang, Z. Y.; Li, M. H. Solubility of carbon dioxide in the solvent system (2-amino-2-methyl-1-propanol + sulfolane + water). *Fluid Phase Equilib.* **2010**, *291* (2), 195−200.

(8) Saha, A. K.; Bandyopadhyay, S. S.; Biswas, A. K. Kinetics of absorption of CO_2 into aqueous solutions of 2-amino-2-methyl-1-propanol. *Chem. Eng. Sci.* **1995**, *50* (22), 3587−3598.

(9) Park, J.-Y.; Yoon, S. J.; Lee, H.; Yoon, J.-H.; Shim, J.-G.; Lee, J. K.; Min, B.-Y.; Eum, H.-M. Density, viscosity, and solubility of CO_2 in aqueous solutions of 2-amino-2-hydroxymethyl-1,3-propanediol. *J. Chem. Eng. Data* **2002**, *47* (4), 970−973.

(10) Park, J.-Y.; Yoon, S. J.; Lee, H.; Yoon, J.-H.; Shim, J.-G.; Lee, J. K.; Min, B.-Y.; Eum, H.-M.; Kang, M. C. Solubility of carbon dioxide in aqueous solutions of 2-amino-2-ethyl-1,3-propanediol. *Fluid Phase Equilib.* **2002**, *202* (2), 359−366.

(11) Le Tourneux, D.; Iliuta, I.; Iliuta, M. C.; Fradette, S.; Larachi, F. Solubility of carbon dioxide in aqueous solutions of 2-amino-2-hydroxymethyl-1,3-propanediol. *Fluid Phase Equilib.* **2008**, *268* (1−2), 121−129.

(12) Klamt, A. Conductor-like screening model for real solvents: A new approach to the quantitative calculation of solvation phenomena. *J. Phys. Chem.* **1995**, *99* (7), 2224−2235.

(13) (a) Yadav, R.; Labhsetwar, N.; Kotwal, S.; Rayalu, S. Single enzyme nanoparticle for biomimetic CO_2 sequestration. *J. Nanopart. Res.* **2011**, *13* (1), 263−271. (b) Mirjafari, P.; Asghari, K.; Mahinpey, N. Investigating the application of enzyme carbonic anhydrase for CO_2 sequestration purposes. *Ind. Eng. Chem. Res.* **2007**, *46* (3), 921−926. (c) Liu, N.; Bond, G. M.; Abel, A.; McPherson, B. J.; Stringer, J. Biomimetic sequestration of CO_2 in carbonate form: Role of produced waters and other brines. *Fuel. Process. Technol.* **2005**, *86* (14−15), 1615−1625.

(14) Mahinpey, N.; Asghari, K.; Mirjafari, P. Biological sequestration of carbon dioxide in geological formations. *Chem. Eng. Res. Des.* **2011**, *89* (9), 1873−1878.

(15) Chiu, H.-Y.; Jung, R.-F.; Lee, M.-J.; Lin, H.-M. Vapor−liquid phase equilibrium behavior of mixtures containing supercritical carbon dioxide near critical region. *J. Supercrit. Fluids* **2008**, *44* (3), 273−278.
(16) Schäfer, A.; Klamt, A.; Sattel, D.; Lohrenz, J. C. W.; Eckert, F. COSMO implementation in TURBOMOLE: Extension of an efficient quantum chemical code towards liquid systems. *Phys. Chem. Chem. Phys.* **2000**, *2* (10), 2187−2193.
(17) Schäfer, A.; Huber, C.; Ahlrichs, R. Fully optimized contracted Gaussian basis sets of triple zeta valence quality for atoms Li to Kr. *J. Chem. Phys.* **1994**, *100* (8), 5829−5835.
(18) Eichkorn, K.; Treutler, O.; Öhm, H.; Häser, M.; Ahlrichs, R. Auxiliary basis sets to approximate Coulomb potentials (Chem. Phys. Letters 240 (1995) 283−290). *Chem. Phys. Lett.* **1995**, *242* (6), 652−660.
(19) Becke, A. D. Density-functional exchange-energy approximation with correct asymptotic behavior. *Phys. Rev. A* **1988**, *38* (6), 3098−3100.
(20) Klamt, A.; Jonas, V.; Bürger, T.; Lohrenz, J. C. W. Refinement and parametrization of COSMO-RS. *J. Phys. Chem. A* **1998**, *102* (26), 5074−5085.
(21) Klamt, A.; Diedenhofen, F. E. M.; Beck, M. E. First principles calculations of aqueous p*K*a values for organic and inorganic acids using COSMO-RS reveal an inconsistency in the slope of the p*K*a scale. *J. Phys. Chem. A* **2003**, *107*, 9380−9386.
(22) Frisch, M. J.; Trucks, G. W.; Schlegel, H. B.; Scuseria, G. E.; Robb, M. A.; Cheeseman, J. R.; Scalmani, G.; Barone, V.; Mennucci, B.; Petersson, G. A.; Nakatsuji, H.; Caricato, M.; Li, X.; Hratchian, H. P.; Izmaylov, A. F.; Bloino, J.; Zheng, G.; Sonnenberg, J. L.; Hada, M.; Ehara, M.; Toyota, K.; Fukuda, R.; Hasegawa, J.; Ishida, M.; Nakajima, T.; Honda, Y.; Kitao, O.; Nakai, H.; Vreven, T.; Montgomery, J. A., Jr.; Peralta, J. E.; Ogliaro, F.; Bearpark, M.; Heyd, J. J.; Brothers, E.; Kudin, K. N.; Staroverov, V. N.; Kobayashi, R.; Normand, J.; Raghavachari, K.; Rendell, A.; Burant, J. C.; Iyengar, S. S.; Tomasi, J.; Cossi, M.; Rega, N.; Millam, N. J.; Klene, M.; Knox, J. E.; Cross, J. B.; Bakken, V.; Adamo, C.; Jaramillo, J.; Gomperts, R.; Stratmann, R. E.; Yazyev, O.; Austin, A. J.; Cammi, R.; Pomelli, C.; Ochterski, J. W.; Martin, R. L.; Morokuma, K.; Zakrzewski, V. G.; Voth, G. A.; Salvador, P.; Dannenberg, J. J.; Dapprich, S.; Daniels, A. D.; Farkas, Ö.; Foresman, J. B.; Ortiz, J. V.; Cioslowski, J.; Fox, D. J., *Gaussian 09*; Gaussian, Inc.: Wallingford, CT, 2009.
(23) Kent, R. L.; Eisenberg, B. Better data for amine treating. *Hydrocarbon Process* **1976**, *55*, 87−90.
(24) Gangarapu, S.; Marcelis, A. T. M.; Zuilhof, H. Improving the capture of CO_2 by substituted monoethanolamines: Electronic effects of fluorine and methyl substituents. *ChemPhysChem* **2012**, *13*, 3973−3980.
(25) Taha, M.; Gupta, B. S.; Lee, M.-J. Complex equilibria in aqueous solutions of chromium (III) with some biological pH buffers. *J. Chem. Eng. Data* **2011**, *56* (9), 3541−3551.
(26) Rudolph, W. W.; Irmer, G.; Konigsberger, E. Speciation studies in aqueous HCO_3−CO_3^{2-} solutions. A combined Raman spectroscopic and thermodynamic study. *Dalton Trans.* **2008**, *7*, 900−908.
(27) (a) Yamada, H.; Matsuzaki, Y.; Chowdhury, F.; Higashii, T. Computational investigation of carbon dioxide absorption in alkanolamine solutions. *J. Mol. Model.* **2013**, *19* (10), 4147−4153. (b) Yamada, H.; Matsuzaki, Y.; Okabe, H.; Shimizu, S.; Fujioka, Y. Quantum chemical analysis of carbon dioxide absorption into aqueous solutions of moderately hindered amines. *10th Int. Conf. Greenhouse Gas Control Technol.* **2011**, *4*, 133−139. (c) Matsuzaki, Y.; Yamada, H.; Chowdhury, F. A.; Higashii, T.; Onoda, M. Ab Initio study of CO_2 capture mechanisms in aqueous monoethanolamine: Reaction pathways for the direct interconversion of carbamate and bicarbonate. *J. Phys. Chem. A* **2013**, *117* (38), 9274−9281. (d) Iida, K.; Sato, H. Proton transfer step in the carbon dioxide capture by monoethanol amine: A theoretical study at the molecular level. *J. Phys. Chem. B* **2012**, *116* (7), 2244−2248. (e) Xie, H.-B.; Johnson, J. K.; Perry, R. J.; Genovese, S.; Wood, B. R. A computational study of the heats of reaction of substituted monoethanolamine with CO_2. *J. Phys. Chem. A* **2011**, *115* (3), 342−350. (f) Han, B.; Zhou, C.; Wu, J.; Tempel, D. J.; Cheng, H. Understanding CO_2 capture mechanisms in aqueous monoethanolamine via first principles simulations. *J. Phys. Chem. Lett.* **2011**, *2*, 522−526. (g) Yamada, H.; Matsuzaki, Y.; Higashii, T.; Kazama, S. Density functional theory study on carbon dioxide absorption into aqueous solutions of 2-amino-2-methyl-1-propanol using a continuum solvation model. *J. Phys. Chem. A* **2011**, *115*, 3079−3086.
(28) (a) Jones, L. H.; McLaren, E. Infrared absorption spectra of SO_2 and CO_2 in aqueous solution. *J. Chem. Phys.* **1958**, *28* (5), 995−995. (b) Riepe, M. E.; Wang, J. H. Infrared studies on the mechanism of action of carbonic anhydrase. *J. Biol. Chem.* **1968**, *243* (10), 2779−2787. (c) Sowa, S.; Towill, L. E. Infrared spectroscopy of plant cell cultures: Noninvasive measurement of viability. *Plant Physiol.* **1991**, *95* (2), 610−615.
(29) Oliver, B. G.; Davis, A. R. Vibrational spectroscopic studies of aqueous alkali metal bicarbonate and carbonate solutions. *Can. J. Chem.* **1973**, *51* (5), 698−702.
(30) (a) Richner, G.; Puxty, G. Assessing the chemical speciation during CO_2 absorption by aqueous amines using in situ FTIR. *Ind. Eng. Chem. Res.* **2012**, *51* (44), 14317−14324. (b) Archane, A.; Fürst, W.; Provost, E. Influence of poly(ethylene oxide) 400 (PEG400) on the absorption of CO_2 in diethanolamine (DEA)/H_2O systems. *J. Chem. Eng. Data* **2011**, *56* (5), 1852−1856.